VERSITA

Central European Journal of Physics
DOI: 10.2478/s11534-006-0036-8
Research article
CEJP 5(1) 2007 25–34

Ab-initio calculation of band structure and linear optical properties of SbSI in para- and ferroelectric phases

Harun Akkus*, Amirullah M. Mamedov†

Department of Physics,
Cukurova University,
01330 Adana, Turkey

Received 28 August 2006; accepted 12 October 2006

Abstract: An ab-initio pseudopotential calculation has been performed by using density functional methods within the local density approximation (LDA) to investigate the band structure and optical properties of the ferroelectric-semiconductor SbSI in the para- and ferroelectric phases. It has been shown that SbSI has an indirect gap in both phases (1.45 eV and 1.49 eV in the para- and ferroelectric phases respectively) and that the smallest direct gap is at the S point of the Brillouin zone (1.56 eV and 1.58 eV in the para- and ferroelectric phases respectively). Furthermore, it is shown that first-order phase transition, from the paraelectric phase to the ferroelectric phase (the transiton temperature is about 22 ^{o}C), does not change the nature of the band gap. Moreover, the linear frequency dependent dielectric function, including self-energy effects, has been calculated along the *c*-polar axis in the para- and ferroelectric phases.

Keywords: SbSI, band structure, optical properties
PACS (2006): 31.15.Ar; 71.20.–b; 77.84.–s; 78.20.Ci; 71.15.Dx

1 Introduction

Antimony sulpho-iodide (SbSI), a member of the group of $A^5B^6C^7$ (A= Sb, Bi, As; B= S, Se, O; C= I, Br, Cl) compounds, has been attractive for its interesting electronic and optical properties. According to Dönges [1] the crystal structure of SbSI is orthorhombic. The point group of SbSI is *mmm* (space group D_{2h}^{16}) in the paraelectric phase above the

* E-mail: hakkus@cu.edu.tr
† E-mail: mamedow@cu.edu.tr

Curie point and *mm2* (space group C_{2v}^9) in the ferroelectric phase below the Curie point. Nitsche and Merz [2] have reported that SbSI is a photoconductor with a maximum sensitivity at 6300-6400 $A°$. Fatuzzo et al [3] have reported that SbSI has ferroelectricity and its Curie point is 22 $C°$.

The crystal structure of SbSI is shown in Fig. 1. This crystal has four SbSI molecules in a unit cell. Each molecule of SbSI extends chain-like along the *c*-axis which is also the polarization axis. Atomic positions in the unit cell are given in Table 1. The Sb and S atoms shift along the polar *c*-axis below the Curie point with respect to iodine by about 0.2 $A°$ and 0.05 $A°$ respectively [4]. Displacements of the Sb and S are shown in Fig. 2 and have proved the phase transition is the displacive type and also first-order.

Table 1 Atomic positions of each atom in the unit cell of SbSI [4].

α	Para (35 °C)			Ferro (5 °C)		
	X_α	Y_α	Z_α	X_α	Y_α	Z_α
Sb	0.119	0.124	0.250	0.119	0.124	0.298
S	0.840	0.050	0.250	0.843	0.049	0.261
I	0.508	0.828	0.250	0.508	0.828	0.250

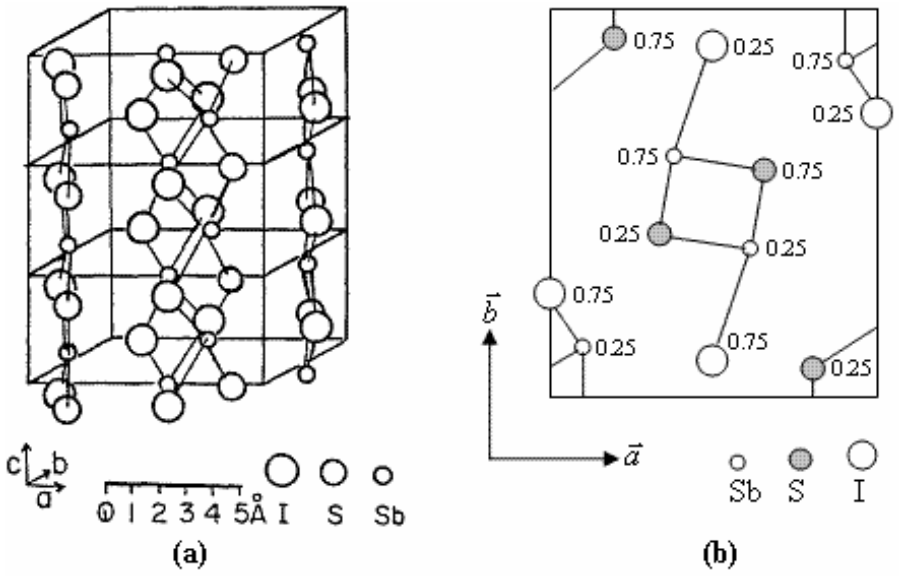

Fig. 1 Crystal structure of SbSI (a); schematic projection of the SbSI molecules on the *xy*-plane in the paraelectric phase (b).

The band structure of SbSI has been investigated by using semiempirical [5], empirical [6], and ab-initio [7] pseudopotential methods. The band structure of SbSI given in Ref. [5, 6] was calculated in the para- and ferroelectric phases but that given in Ref. [7] was only calculated in the paraelectric phase. So in the literature there is no ab-initio calculation based on the ab-initio pseudopotential method of band structure of SbSI in the ferroelectric phase. Furthermore, optical properties of SbSI have been widely

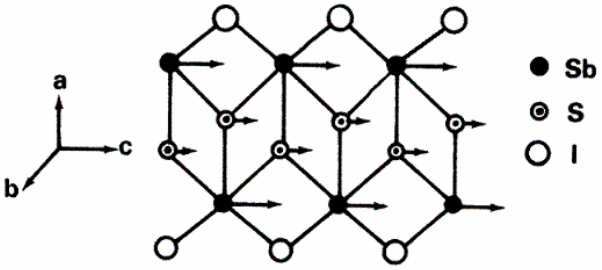

Fig. 2 Atomic displacements from the paraelectric phase to the ferroelectric phase.

studied [5, 8–14] since the 1960s due to its semiconducting and ferroelectric properties but calculations of the optical properties of SbSI based on the first-principle pseudopotential method are absent in the literature.

In this paper, we have investigated and calculated electronic and optical properties of SbSI in the para- and ferroelectric phases by using the pseudopotential method based on the density functional theory (DFT) in the local density approximation (LDA) [15].

2 Details of ab-initio calculations of the band structure and optical properties of SbSI

The self consistent norm-conserving pseudopotentials were generated by using FHI98PP code [16] with the Troullier-Martins scheme [17]. Plane waves were used as basis set for the electronic wave functions. In order to solve the Kohn-Sham equations [15], the conjugate gradient minimization method [18] was employed by the ABINIT code [19]. The exchange-correlation effects were taken into account within the Perdew-Wang (PW92) sceheme [20] in the LDA in the pseudopotential and the band structure calculations. For Sb and I atoms the 5s and 5p electrons, and for the S atom the 3s and 3p electrons were considered as the true valence.

All the calculations involve a 12 atom orthorhombic unit cell. We have got a good convergence for the bulk total-energy calculation with the choice of cutoff energies at 12 Hartree using the $4 \times 4 \times 4$ Monkhorst-Pack [21] mesh grid. We have found that in the band structure calculations 64 **k** points are enough to obtain good results for SbSI. In the optical properties calculations, however, the irreducible Brillouin zone (BZ) has been sampled with a $24 \times 24 \times 24$ Monkhorst-Pack grid for SbSI.

It is well known that the effect of electric field vector $\vec{E}(\omega)$ of the incoming light is to polarize the material. At the level of linear response this polarization can be calculated using the following relation [22]

$$P^i(\omega) = \chi^{(1)}_{ij}(-\omega, \omega) \cdot \vec{E}^j(\omega) \tag{1}$$

where $\chi^{(1)}_{ij}$ is the linear optical susceptibility tensor and is given by [22, 23]

$$\chi^{(1)}_{ij}(-\omega, \omega) = \frac{e^2}{\hbar\Omega} \sum_{nm\vec{k}} f_{nm}(\vec{k}) \frac{r^i_{nm}(\vec{k})\, r^j_{mn}(\vec{k})}{\omega_{mn}(\vec{k}) - \omega} = \frac{\varepsilon_{ij}(\omega) - \delta_{ij}}{4\pi} \tag{2}$$

where n, m denote energy bands, $f_{mn}(\vec{k}) \equiv f_m(\vec{k}) - f_n(\vec{k})$ is the Fermi occupation factor, Ω is the normalization volume. $\omega_{mn}(\vec{k}) \equiv \omega_m(\vec{k}) - \omega_n(\vec{k})$ is the frequency difference, $\hbar\omega_n(\vec{k})$ is the energy of band n at wave vector $\mathbf{k}$. The $\vec{r}_{nm}$ are the matrix elements of the position operator and are given by [23]

$$\begin{aligned} r^i_{nm}(\vec{k}) &= \tfrac{v^i_{nm}(\vec{k})}{i\omega_{n\,m}}\,; \;\; \omega_n \neq \omega_m \\ r^i_{nm}(\vec{k}) &= 0 \qquad\quad ; \;\; \omega_n = \omega_m \end{aligned} \tag{3}$$

where $v^i_{nm}(\vec{k}) = m^{-1}p^i_{nm}(\vec{k})$, m is the free electron mass, and $\vec{p}_{nm}$ is the momentum matrix element.

As can be seen from Eq. (2) dielectric function $\varepsilon_{ij}(\omega) = 1 + 4\pi\chi^{(1)}_{ij}(-\omega,\omega)$ and the imaginary part of $\varepsilon_{ij}(\omega)$, $\varepsilon^{ij}_2(\omega)$ is given by

$$\varepsilon^{ij}_2(\omega) = \frac{e^2}{\hbar\pi}\sum_{nm}\int d\vec{k}\, f_{nm}(\vec{k})\frac{v^i_{nm}(\vec{k})v^j_{mn}(\vec{k})}{\omega^2_{mn}}\delta(\omega - \omega_{mn}(\vec{k})). \tag{4}$$

The real part of $\varepsilon_{ij}(\omega)$, $\varepsilon^{ij}_1(\omega)$ can be obtained by using the Kramers-Kronig transformation

$$\varepsilon^{ij}_1(\omega) - 1 = \frac{2}{\pi}\,\wp\int_0^\infty \frac{\omega'\,\varepsilon^{ij}_2(\omega')}{\omega'^2 - \omega^2}\,d\omega'. \tag{5}$$

Because the Kohn-Sham equations determine ground-state properties, the unoccupied conduction bands which appear in the calculations have no physical significance. If they are used as single-particle states in a calculation of optical properties for semiconductors, a band gap problem comes into existence: the absorption starts at too low an energy [22]. The many-body effects must be included in calculations of response. In order to take into account self-energy effects, in the present work we used the "scissors approximation" [22, 24].

Within the scissors approximation the Hamiltonian from which response functions are calculated is given by

$$\tilde{H} = H + V_s \tag{6}$$

where

$$H = \frac{p^2}{2m} + V(\vec{r}) - e\,\vec{r}\cdot\vec{E} \tag{7}$$

and

$$V_s = \Delta\sum_{c\vec{k}}\left|c\vec{k}\right\rangle\left\langle c\vec{k}\right| \tag{8}$$

is the scissors operator [22]. In this expression the sum is over all $\mathbf{k}$ and conduction bands c, Δ is the constant energy shift related to the correction of the band gap, and $\left|c\vec{k}\right\rangle$ denotes single-particle eigenstates of the unperturbed Hamiltonian. In the framework of the scissors approximation Eq. (2) can be rewritten as follows

$$\chi^{(1)}_{ij}(-\omega,\omega) = \frac{e^2}{\hbar\Omega}\sum_{nm\vec{k}} f_{nm}(\vec{k})\frac{r^i_{nm}(\vec{k})\,r^j_{mn}(\vec{k})}{\omega_{mn}(\vec{k}) + \frac{\Delta}{\hbar}(\delta_{mc} - \delta_{nc}) - \omega}. \tag{9}$$

The difference between Eqs. (2) and (9) is only the modification of the frequencies ω_{mn}, $\omega_{mn} \rightarrow \frac{\Delta}{\hbar}(\delta_{mc} - \delta_{nc})$.

3 Results and discussion

The notations of the high-symmetry points between which we have drawn the band structure correspond to those chosen in Ref. [25] and they are shown in Fig. 3. The calculated band structures of SbSI in the para- and ferroelectric phases are presented in Fig. 4 and 5 respectively. We have observed the presence of well separated groups of bands in both phases. As previously discussed in Ref. [9, 26], the chemical bonding in SbSI has a mixed covalent-ionic character. According to Ref. [26] the bond between antimony and sulfur atoms in the chain is covalent while the iodine ion in an ionic bond with a covalently bound bridge $(SbS)^+$.

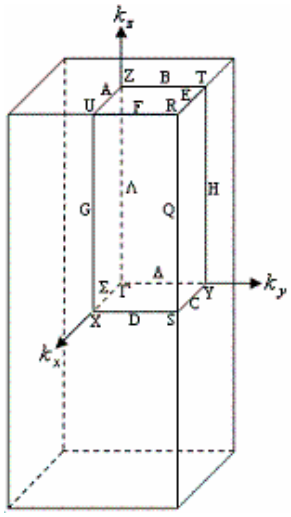

Fig. 3 The first Brillouin zone of the SbSI crystal.

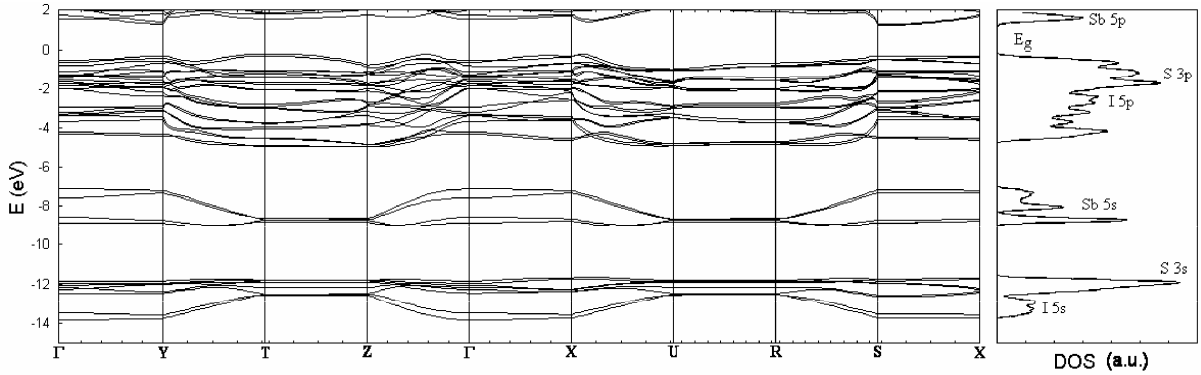

Fig. 4 Band structure and the corresponding total density of states of SbSI in the paraelectric phase (the atomic positions at 35 °C are used in the calculations).

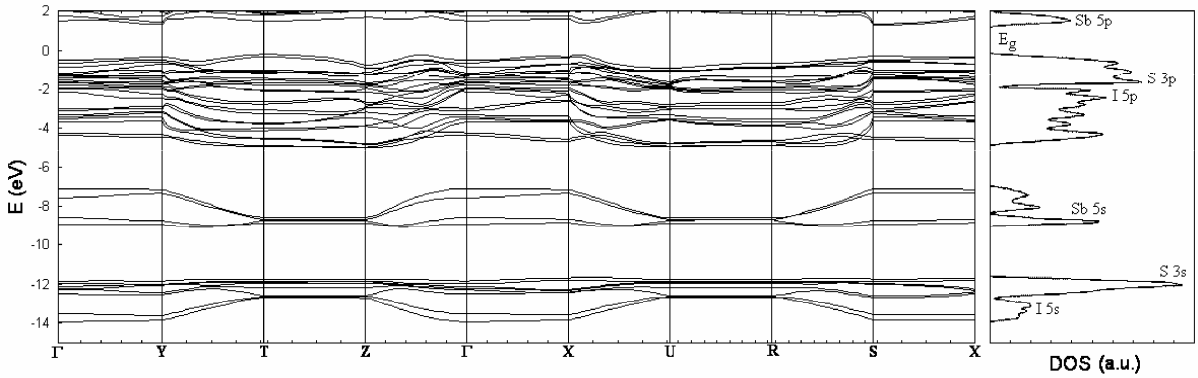

Fig. 5 Band structure and the corresponding total density of states of SbSI in the ferroelectric phase (the atomic positions at 5 °C are used in the calculations).

In Fig. 4 and 5 shown in the rightmost panels are the normalized total density of states (DOS) for the SbSI crystal. The valence band in both phases is composed of the 5s- and 5p-orbitals of the I atom, the 3s- and 3p-orbitals of the S atom, and the 5s-orbitals of the Sb atom, while the conduction band consists of the 5p-orbitals of the Sb atom.

As can be seen in Fig. 4 and 5, the SbSI crystal has an indirect forbidden gap in both phases. The minimum of the conduction band is located at the S point of BZ: 1.24 eV and 1.28 eV in the para- and ferroelectric phases, respectively. The maximum of the valence band is located at the T point of BZ: -0.22 eV and -0.20 eV in the para- and ferroelectric phases, respectively. The value of the forbidden gap is 1.45 eV and 1.49 eV in the para- and ferroelectric phases, respectively ($\Delta E_g = 0.04\,eV$). Our results for the paraelectric phase concide with the data given in Ref. [7, 26] and for the ferroelectric phase partially with the data in Ref [5, 6].

The indirect gap E_g increases from 1.45 eV (T→S) to 2.91 eV (Z→U) and from 1.49 eV (T→S) to 2.80 eV (Z→U) in the para- and ferroelectric phases, respectively. The direct band gap E_g increases from 1.56 eV (at the S point) to 3.11 eV (at the U point) and from 1.58 eV (at the S point) to 2.94 eV (at the U point) in the para- and ferroelectric phases, respectively. The uppermost band of the valence level and the bottom band of the conduction level are presented separately in Fig. 6. As seen in Fig. 6, the first-order phase transition does not change the nature of the band gap.

Because of the orthorhombic crystal symmetry, the linear susceptibility tensor of the the SbSI crystal in both phases has three independent components that are the diagonal elements of the susceptibility tensor [27]. The calculated, by using Eqs. (2), (5), and (9), real and imaginary parts of the *zz* component of the linear frequency dependent dielectric function are presented in Fig. 7 and 8, respectively. The value of $\varepsilon_1^{zz}(\omega)$ calculated by us is equal to zero about 3 eV and 2.95 eV in the para- and ferroelectric phases, respectively. The values of the $\varepsilon_2^{zz}(\omega)$ peaks shown in Fig. 8 are summarized in Table 2. The peaks correspond to the transition from the valence band to the conduction band. Our results concerning the dielectric function for the paraelectric phase are in agreement with the data given in Ref [5, 26] in the low-energy regions.

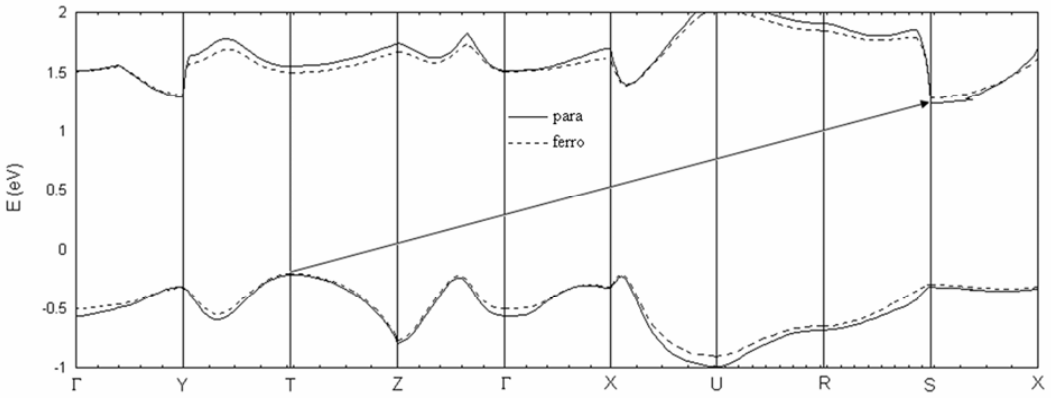

Fig. 6 Diagram of the forbidden band gap variation of the SbSI crystal during the phase transition.

Table 2 Comparative characteristics of the linear optical functions of the SbSI crystal (first-principle calculation).

	Peaks (eV)									
ε_2^{zz}	A	B	C	D	E	F	G	H	I	J
para	1.70	2.05	2.52	2.98	3.30	4.24	4.65	5.48	6.80	-
ferro	1.75	2.07	2.30	2.45	2.88	3.32	4.12	4.55	4.90	6.20

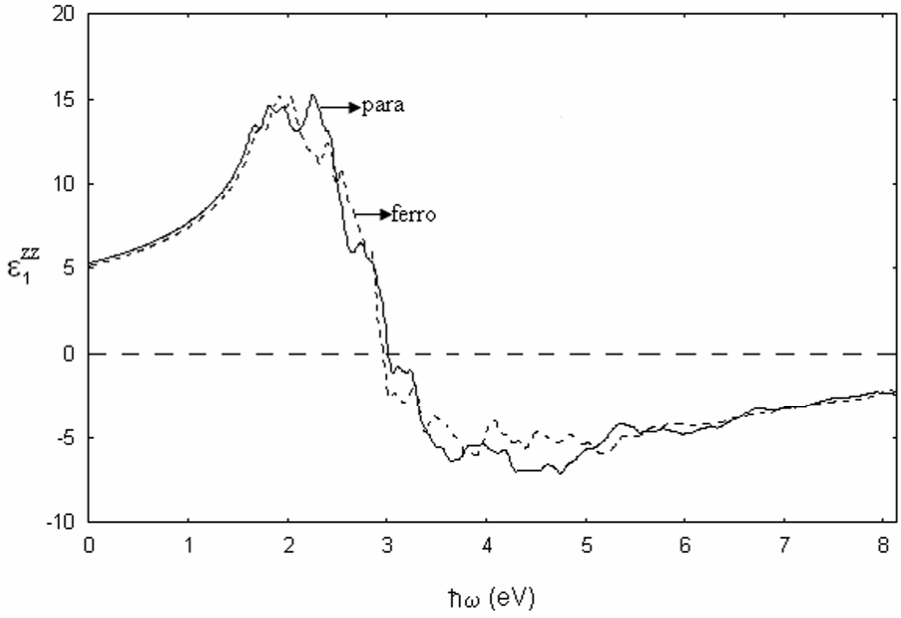

Fig. 7 Real parts of the *zz*-component of the linear dielectric tensor in the para- and ferroelectric phases.

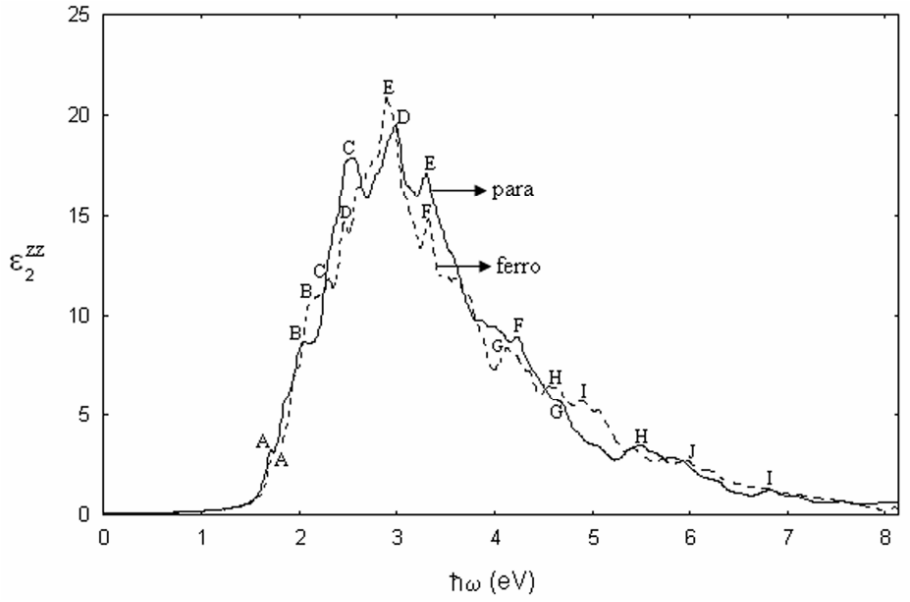

Fig. 8 Imaginary parts of the *zz*-component of the linear dielectric tensor in the para- and ferroelectric phases.

4 Conclusions

In this work, the electronic band structure and the linear optical properties of SbSI have been calculated by the ab-initio pseudopotential method in the para- and ferroelectric phases. Our aim was to apply the density functional methods to the ferroelectric-semiconductor SbSI. The SbSI crystal has an indirect forbidden gap in both phases and has the smallest direct gap at the S point of the Brillouin zone. The 3p-orbitals of the sulfur atom consitute the valence band top, and the bottom of the conduction band is composed of the 5p-orbitals of the antimony atom in both phases. The first-order phase transition does not change the character of the band gap, however, it changes the value of the band gap by about 0.04 eV. This change in the band structure of SbSI with the change of symmetry is also related to the availability of spontaneous polarization in the ferroelectric phase. The linear frequency dependent dielectric function along the *c*-polar axis, including self-energy effects, has also been calculated in both phases and is in good agreement with the previous experimental data in the low-energy regions. In summary, it is shown through this work that the density functional methods are suitable for the calculations of the electronic band structure and optical properties of complex crystals like SbSI.

References

[1] E.Z. Dönges: "Chalcogenides of trivalent antimony and bismuth. I. Thiohalides of trivalent antimony and bismuth", *Z. Anorg. Chem.*, Vol. 263, (1950), pp. 112–132; "Über Chalkogenohalogenide des dreiwertigen Antimons und Wismuts. III. Über

Tellurohalogenide des dreiwertigen Antimons und Wismuts und über Antimon-und Wismut(III)-tellurid und Wismut(III)-selenid", *Z. Anorg. Chem.*, Vol. 265, (1951), pp. 56–61.

[2] R. Nitsche and W.J. Merz: "Photoconduction in ternary V-VI-VII compounds", *J. Phys. Chem. Solids,* Vol. 13, (1960), pp. 154–155.

[3] E. Fattuzo, G. Harbeke, W.J. Merz, R. Nitsche, H. Roetschi and W. Ruppel: "Ferroelectricity in SbSI", *Phys. Rev.,* Vol. 127, (1962), pp. 2036–2037.

[4] A. Kikuchi, Y. Oka and E. Sawaguchi: "Crystal structure determination of SbSI", *J. Phys. Soc. Jap.,* Vol. 23, (1967), pp. 337–354.

[5] K. Nakao and M. Balkanski: "Electronic Band Structures of SbSI in the Para- and Ferroelectric Phases", *Phys. Rev. B*, Vol. 8, (1973), pp. 5759–5780.

[6] A. Audzijonis, R. Zaltauskas, L. Audzijoniene, I.V. Vinokurova, O.V. Farberovich and R. Sadzius: "Electronic Band Structure of Ferroelectric Semiconductor SbSI Studied by Empirical Pseudopotential", *Ferroelectrics,* Vol. 211, (1998), pp. 111–126.

[7] D.M. Bercha, K.Z. Rushchanskii, M. Sznajder, A. Matkovskii and P. Potera: "Elementary energy bands in ab initio calculations of the YAlO3 and SbSI crystal band structure", *Phys. Rev. B*, Vol. 66, (2002), art. 195203.

[8] Y. Masuda, K. Sakata, S. Hasegawa, G. Ohara, M. Wada and M. Nishizawa: "Growth and Some Electrical Properties of Orientated Fibriform Crystal of SbSI", *Jap. J. Appl. Phys.*, Vol. 8, (1969), pp. 692–699.

[9] E.I. Gerzanich, V.A. Lyakhovitskaya, V.M. Fridkin and B.A. Popovkin: "SbSI and other ferroelectric $A^{V}B^{VI}C^{VII}$ materials", In: E. Kaldis (Ed.): *Current topics in materials science*, Nort-Holland Publishing Company, Amsterdam, New York and Oxford, 1982, pp. 55–190.

[10] K. Toyoda: "Electrical Properties of SbSI Crystals In The Vicinity of the Ferroelectric Curie Point", *Ferroelectrics.*, Vol. 69, (1986), pp. 201–215.

[11] L.E. Cross, A. Bhalla, F. Ainger and D. Damjakovic: *Pyro-optic detector and Imajer*, US Patent No. 4994. 672, 1991.02.19.

[12] A.M. Mamedov: "Nonlinear optical properties of SbSI", *Sov. Phys. Solid State,* Vol. 19, (1977), 845-858 (in Russian).

[13] S. Surthi, S. Kortu and R.K. Pandey: "Preparation and electrical properties of ferroelectric SbSI films by pulsed laser deposition", *J. Mat. Sci. Lett.*, Vol. 22, (2003), pp. 591–593.

[14] A.M. Mamedov, A.O. Aliev, B.M. Kasumov and S.M. Efendiev: "The Optical Properties of SbSI in The Fundamental Absorbtion Region", *Ferroelectrics,* Vol. 83, (1988), pp. 157–159.

[15] W. Kohn and L.J. Sham: "Self-Consistent Equations Including Exchange and Correlation Effects", *Phys. Rev.,* Vol. 140, (1965), pp. A1133–1138.

[16] M. Fuch and M. Scheffler: "Ab initio pseudopotentials for electronic structure calculations of poly-atomic systems using density-functional theory", *Comput. Phys. Commun.*, Vol. 119, (1999), pp. 67–98.

[17] N. Troullier and J.L. Martins: "Efficient pseudopotentials for plane-wave calculations", *Phys. Rev. B*, Vol. 43, (1991), pp. 1993–2006.

[18] M.C. Payne, M.P. Teter, D.C Allan, T.A. Arias and J.D. Joannopoulos: "Iterative minimization techniques for ab initio total-energy calculations: molecular dynamics and conjugate gradients" *Rev. Mod. Phys.*, Vol. 64, (1992), pp. 1045–1097.

[19] X. Gonze, J.M. Beuken, R. Caracas, F. Detraux, M. Fuchs, G.M. Rignanese, L. Sindic, M. Verstrate, G. Zerah, F. Jollet, M. Torrent, A. Roy, M. Mikami, P. Ghosez, J.Y.Raty and D.C. Allan: "First-principles computation of material properties : the ABINIT software project", *Computational Materials Science*, Vol. 25, (2002), pp. 478–492, http://www.abinit.org.

[20] J.P. Perdew and Y. Wang: "Accurate and simple analytic representation of the electron-gas correlation energy", *Phys. Rev. B.*, Vol. 45, (1992), pp. 13244–13249.

[21] H.J. Monkhorst and J.D. Pack: "Special Points for Brillouin-zone Integrations", *Phys. Rev. B*, Vol. 13, (1976), pp. 5188–5192.

[22] J.L.P. Hughes and J.E. Sipe: "Calculation of second-order optical response in semiconductors", *Phys. Rev. B*, Vol. 53, (1996), pp. 10751–10763.

[23] S. Sharma and C. Ambrosch-Draxl: "Second-order Optical Response From First Principles", *Physica Scripta.*, Vol. T109, (2004), pp. 128–135.

[24] Z.H. Levine and D.C. Allan: "Linear optical response in silicon and germanium including self-energy effects", *Phys. Rev. Lett.,* Vol. 63, (1989), pp. 1719–1722.

[25] O.V. Kovalev: "Representations of the Crystallographic Space Groups", In: H.T. Stokes and D.M. Hatch (Ed.): *Irreducible Representations, Induced Representations and Corepresentations*, 2nd ed., Gordon and Breach Science Publishers, Amsterdam, 1993.

[26] J.F. Alward, C.Y. Fong, M. El-Batanouny and F. Wooten: "Electronic and optical properties of SbSBr, SbSI and SbSeI", *Solid State Com.*, Vol. 25, (1978), pp. 307–311.

[27] J.F. Nye: *Physical Properties of Crystals,* Clarendon Press, Oxford, 1957.